In Search for Structure of Active Site in Iron-Based Oxygen Reduction Electrocatalysts

Manish Jain,* Shih-hung Chou, and Allen Siedle

Corporate Materials Research Laboratory, 3M Company, St. Paul, Minnesota 55144

Received: October 11, 2005; In Final Form: December 22, 2005

Calculations to elucidate the structure of Fe-based electrocatalysts were performed. Lowest energy configurations for incorporation of nitrogen in bulk of graphene sheet as well as on edge were determined. Substitution of nitrogen in bulk graphene is endothermic, while on the edge it can be either exothermic, if hydrogen is present, or endothermic. Energies of various configurations for the incorporation of iron on the edge of the nitrided graphene sheet were also examined. In the absence of hydrogen, iron prefers to bond with nitrogen and a carbon atom. In the presence of hydrogen, however, iron was found to prefer bonding to two nitrogen atoms on the graphene edge.

I. Introduction

Fuel cells are devices that transform chemical reaction energy into electrical energy. They have attracted much interest in the context of distributed global energy needs as well as localized power sources for appliances such as laptop computers. A critical but complex cathodic process in a functioning proton-exchange membrane fuel cell is the electrochemical reduction of oxygen (eq 1)

$$O_2 + 4H^+ + 4e^- \rightarrow 2H_2O \qquad (1)$$

Much effort has been devoted to elucidating the mechanism of this reaction, which is incompletely understood even on seemingly simple platinum single-crystal surfaces.[1] Another more practically and economically driven aspect of oxygen reduction reaction (ORR) electrochemistry has been a search for less expensive yet effective substitutes for platinum, currently the electrode material of choice. One, centered on iron, was of interest because we considered that the fundamental chemistry might be carried out using continuous, vacuum sputtering deposition process technology.[2] The progress in this nonprecious metal ORR catalysts area during the past 10 years can be followed through the effort by Dodelet's group.[3] For example, Lefèvre and co-workers[4] prepared oxygen reduction electrode materials by pyrolyzing perylenetetracarboxylic dianhydride combined with various Fe and N precursors. From secondary ion mass spectrometric (SIMS) studies, the authors proposed that the ion fragment $FeN_2C_4^+$ might be a signature of the most active catalytic site. This result has led to the suggestion that the active site might correspond to a graphene lattice into which Fe and N had been substituted and in which the nitrogen atoms act as ligands that provide binding sites for iron.

In the literature, there have been several studies—both experimental and theoretical—of incorporation of nitrogen atoms in carbon solid-state structures.[5−13] Merchant et al.[5] have considered structures generated by cathodic arc deposition of nitrided carbon films. Stafstrom[6] has examined incorporation of nitrogen atoms into fullerene-like structures. Jungnickel et al.[9] have studied doping of nitrogen in sp^2 forms of carbon. Dos Santos and Alvarez[14] investigated the structural evolution of a graphene sheet as increasing amounts of nitrogen were substituted. A transition from planar to corrugated topology was calculated to occur at relative atomic concentration [N]/[C] > 20%. In this study, the purpose is to examine the ORR catalyst system as proposed by Dodelet[4] using graphene sheets containing small amounts of nitrogen. Experimentally, these low levels of nitrogen were usually introduced in a high-temperature pyrolysis reaction of the catalyst precursor in the presence of ammonia.

Synthesis of catalytic materials using continuous vacuum sputtering processes[2] can be achieved in both the presence and absence of hydrogen. Nitrogen gas can serve as the source of nitrogen as opposed to ammonia. The role of hydrogen in these materials has not been studied.

The high-temperature synthesis condition in Dodelets' work and others in this area[15] raises the possibility that the system may be under thermodynamic control. While kinetics might play an important role in growth of nitrided graphene, it will not be considered in this study. To gain understanding of Fe−C−N ORR electrocatalysts, we first examined energetics of incorporation of nitrogen in planar graphene sheets. All studies were undertaken in both the presence and absence of hydrogen. One of the goals of this study was to identify sites that two nitrogen atoms could occupy—edge sites or interior positions. It was of interest to find out whether nitrogen edge site substitution is preferred than graphene interior site substitution. It was also of interest to identify the lowest energy substitution sites that two nitrogen atoms would prefer—adjacent positions (with N−N bonds) or ortho, meta, or para positions relative to each other.

Subsequently, we also investigated the interaction of a single iron atom with the various graphene edge structures, with two carbon atoms on the edge substituted by two nitrogen atoms. The purpose was to identify most energetically favorable FeN_2C_4 ORR catalyst structure and compare its energy of formation to the structure proposed by Dodelet and co-workers.[4]

II. Computational Methods

To calculate the stability of various configurations of nitrogen and iron atoms in graphite, total energy calculations using the density functional theory (DFT) method with periodic boundary conditions were performed. The ab initio calculations within DFT were carried out using generalized gradient approximation

* Corresponding author. E-mail: mjain@mmm.com.

10.1021/jp055799l CCC: $33.50
Published on Web 02/10/2006

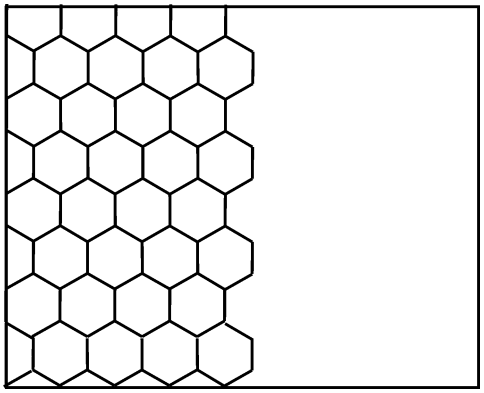

Figure 1. Graphene edge considered in the calculations. A row of atoms is eight atoms along the edge.

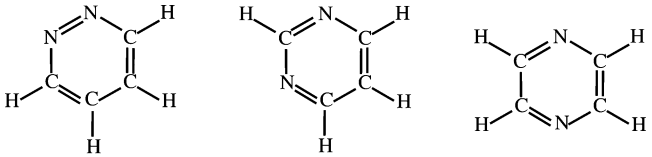

Figure 2. Isomers of diazines: (a) 1,2-diazine (ortho), (b) 1,3-diazine (meta), and (c) 1,4-diazine (para).

of Perdew and Wang (PW91)[16] for the exchange correlation functional. This was used as implemented via the Vienna ab-initio simulation package (VASP).[17−19] Projector augmented waves (PAW)[20] were used to represent the valence electrons of carbon, nitrogen, and iron. The interaction between the basal planes of graphite is of weak van der Waals type. It is poorly described within DFT and was completely ignored in this calculation. Calculations were performed for graphene sheets within the supercell geometry with a spacing of 10 Å between sheets. This spacing ensured that there was negligible interaction between the layers. Four points were sampled in the Brillouin zone to properly account for the metallic nature of graphene. The results did not change significantly upon going to a higher *k* point sampling. The dimensions of the sheet were 19.1 Å by 16.54 Å. This amounted to 128 atoms in the system. All atoms were allowed to relax to their minimum-energy positions such that the force on any atom was less than 0.01 eV/Å.

To model an edge of graphite, the graphene sheets were cut along an armchair edge so that there were 80 atoms in the system (as shown in Figure 1). Within the periodic DFT code, two *k* points were sampled in the Brillouin zone along the continuous direction to account for the metallicity of graphene in that direction. Several rows of atoms from the edge were allowed to relax to their equilibrium positions. Forces on the relaxed atoms in all cases were minimized to less than 0.01 eV/Å.

To examine the suitability of the PAW potentials, structural properties of pure graphite were calculated. The carbon−carbon bond distance corresponding to lowest energy was 1.41 Å. This is in good agreement with the experimental value[21] of 1.42 Å. The interlayer spacing was calculated to be 3.31 Å compared to 3.35 Å in experiment. While interlayer spacing is close to the experimental value, the inadequacy of present density functionals to describe the van der Waal interactions is well-known. These calculations agree with other density functional calculations[22] on graphite.

To further test the potentials within DFT, the relative stabilities of the three $C_4H_4N_2$ diazine isomers were examined (shown in Figure 2). This calculation was done in a large supercell of size 20 Å in each direction. Only the gamma point was sampled for these calculations.

TABLE 1: Relative Stability of Diazines As Calculated Using DFT

compound	relative energy (DFT) (eV)	experimental[24] relative stability (eV)
1,3-diazine	0.0	0.0
1,4-diazine	0.16	0.001
1,2-diazine	0.91	0.85

Upon relaxation of the armchair edge of graphene, without hydrogen atoms passivating the surface, bond lengths between atoms at the edge decrease. Because the atoms at the edge are 2-fold coordinated, they shorten their other bonds to reduce their energy. The bond lengths between two such 2-fold coordinated atoms contracts to 1.24 Å forming a triple bond as compared to 1.41 Å in the bulk. Their bonds with 3-fold carbon atoms also shorten, and their bond length contracts to 1.34 Å. This is in good agreement with previous calculations.[23]

In the presence of hydrogen, it was found that the system lowers its energy by acquiring hydrogen atoms at the edge. This is in accordance with the expectation that absent the passivating effect of C−H bond formation, the graphene edge has dangling bonds on the surface, which make it highly reactive.

High-resolution transmission electron microscopy[13] (HREM) revealed that amorphous CN_x films contain buckled and curved basal planes. However, dos Santos et al.[14] have established that the nitrogen-substituted carbon clusters in graphite-like structures are planar for nitrogen concentrations up to [N]/[C] ∼ 20%. The models employed in this study have [N]/[C] ratios which are far smaller than this concentration, and therefore it is reasonable to use planar conformations.

III. Results

Incorporation of Nitrogen in Graphene (in Bulk as Well as on Edge). Table 1 shows the relative stability of diazine isomers. The values are in good agreement with the calculated values available in the literature.[24] For the isomeric diazines, it was found that 1,3-diazine is the most stable isomer. The isomer in which the nitrogen atoms are in the 1,2-position (i.e., adjacent) is higher in energy by 0.91 eV. The 1,4 isomer is also higher in energy with respect to the 1,3 isomer—although only by 0.16 eV. The results from this study are in good qualitative agreement with the experimental trends in the heats of formation of these compounds.[24]

To assess the thermodynamic stability of nitrogen-substituted carbon in a solid-state environment, the incorporation of nitrogen in a graphene sheet was studied. It was found that the energetics of substituting carbon with nitrogen in the bulk of graphene are unfavorable. On substituting one carbon in graphene by nitrogen, the change in energy corresponding to the reaction (ΔE) shown in eq 2 is 0.71 eV.

$$\mathrm{C{:}C} + {}^1/_2\mathrm{N_2} \rightarrow \mathrm{C{:}N} + \mathrm{C_{graphite}} \qquad (2)$$

The energy of substitution is given as

$$\Delta E = E(\text{N-substituted system}) - E(\text{N-unsubstituted system}) + E(\mathrm{C}) - 0.5E(\mathrm{N_2}) \qquad (3)$$

where E(C) is the energy per carbon atom in a graphene sheet. Since this reaction is endothermic, such a substitution is unlikely to happen.

Upon introducing two nitrogen atoms in the bulk, ΔE according to eq 3 becomes position dependent and is given as

$$\Delta E = E(\text{N-substituted system}) - E(\text{N-unsubstituted system}) + 2E(\text{C}) - E(\text{N}_2) \quad (4)$$

Table 2 shows both the relative energies and the energies of substitution for various configurations. The energy is lowest when two nitrogen atoms are far apart and not in the same ring (as configuration a−e shown in Figure 3). It is highest (least favorable) when the nitrogen atoms are adjacent to each other. This calculated trend of energetics for two nitrogen substitutions in a graphene sheet is similar to that found in diazine isomers. As the nitrogen atoms move further apart (from first-nearest neighbors to second-nearest neighbors), the energy of substitution becomes lower. The structure when two nitrogen atoms are in the 1,4-position within the six-membered ring (configuration a−d in Figure 3) is close in energy to the one when nitrogen atoms are far apart (configuration a−e in Figure 3). This indicates that the nitrogen atoms do not interact with each other strongly once they are beyond second-nearest neighbors. It also appears that the interaction between them is repulsive.

The interaction between two nitrogen atoms within a graphene sheet can be examined using the nitrogen 2s partial density of states (DOS) (Figure 4). The splitting of the s level into bonding and antibonding states decreases from 3.25 eV (configuration a−b) to zero (configuration a−e) as the nitrogen atoms are moved away from each other. When they are in the para position in a six-membered ring (configuration a−d), the splitting is less than 1 eV. In all two-nitrogen-atom models considered (for substitution in the bulk), the energy of substitution (ΔE) is endothermic. This type of substitution is not preferred.

Figure 4 compares the partial nitrogen DOS of 2p states for the various graphene models with two nitrogen atoms in the interior sites. It is evident from the figure that nitrogen 2p DOS is not very sensitive to the variation of the nitrogen atoms substitution sites. There is a peak at about 9 eV below the Fermi level. The nitrogen p states in the bulk are delocalized due to hybridization with carbon p states. From Figure 4, one can conclude that the nitrogen substitution site preference is only weakly dependent on the nitrogen 2p states. The nitrogen 2s states, however, are affected strongly by the proximity of the nitrogen atoms.

Figure 5 shows the various configurations when two nitrogen atoms have been substituted at the edge of a graphene sheet. The calculations were done both with and without hydrogen atoms passivating the graphene edge. When the edge is terminated with hydrogen, there are two options. While the carbon atoms on the edge are always passivated by hydrogen atoms, the nitrogen atoms on the edge may or may not be passivated. To assess whether that is the case, we considered the following reaction:

$$\text{C:N(no N−H bonds; Figure 5(ii))} + \text{H}_2 \rightarrow \text{C:N−H(with N−H bonds; Figure 5(iii))} \quad (5)$$

The ΔE for the reaction can be written as

$$\Delta E = E(\text{C:N−H}) - E(\text{C:N}) - E(\text{H}_2) \quad (6)$$

All configurations with different number of hydrogen atoms were compared in this manner. The heat of formation of hydrogen molecule was calculated to be −4.55 eV, which agrees well with the experimental value.[32] It was found that the configurations that have nitrogen atoms passivated by the hydrogen atoms are always lower in energy than their counterparts, where the nitrogen atoms were left unpassivated. This agrees well with experimental data of Bouchet-Fabre et al.[35]

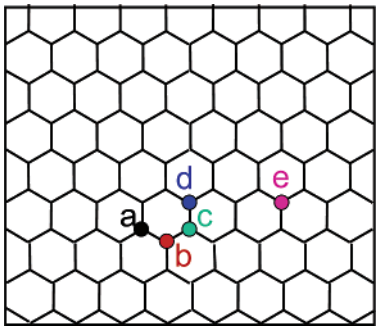

Figure 3. Position of nitrogen atoms in the bulk graphene.

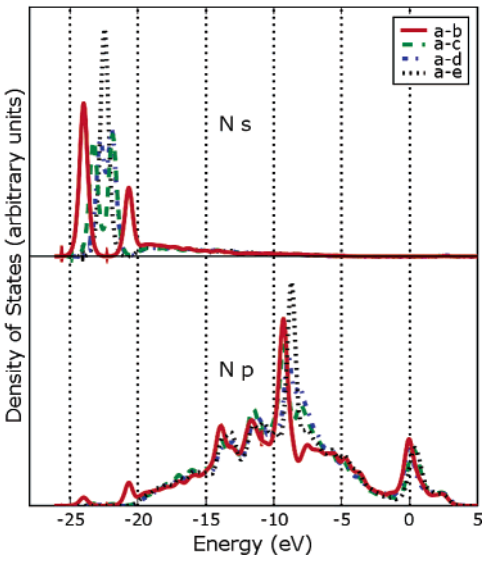

Figure 4. Nitrogen partial density of states for nitrogen substituted in bulk graphene.

TABLE 2: Relative Energies and Heats of Substitution for Two Nitrogen Atoms in the Bulk of a Graphene Sheet (See Figure 3)

positions	relative energy (DFT) (eV)	heat of substitution (DFT) (eV)
a−b	0.0	2.71
a−c	−0.82	1.89
a−d	−1.13	1.58
a−e	−1.17	1.54

The authors[35] there found that, upon incorporating nitrogen in amorphous CN_x:H, C−H vibrations are replaced by N−H vibrations. The heats of reaction for various configurations as calculated according to eq 6 are −0.55 to −0.7 eV. This binding of hydrogen to nitrogen is opposite to the case of pyridine.[33] In pyridine, there is a loss of resonance energy due to the formation of the N−H bond. As the system size becomes large, this resonance energy loss becomes smaller and the penalty for the loss of aromaticity becomes smaller.[34]

In the absence of hydrogen atoms, the graphene sheet undergoes significant relaxation. Figure 6 shows the convergence of total energy as rows of carbon atoms from the graphene edge were relaxed in the absence of hydrogen. Relaxation of atoms in this case extends up to the fourth row of atoms from the edge. The total energy of the system does not decrease significantly beyond that. Table 3 shows the relative stability and energies of substitution of nitrogen atoms for various configurations on the edge of a graphene sheet in both the presence and absence of hydrogen (as calculated using eq 3). In addition to the configurations shown in Figure 5, other configurations—where one of the nitrogen atoms was in a 3-fold

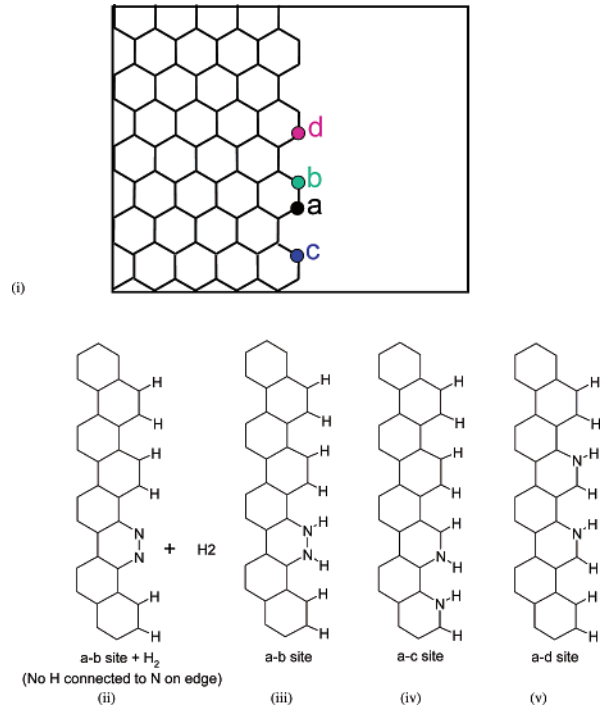

Figure 5. (i) Positions of nitrogen atoms on the edge of graphene. (ii) Shows the attachment of hydrogen atoms to the nitrogen atoms.

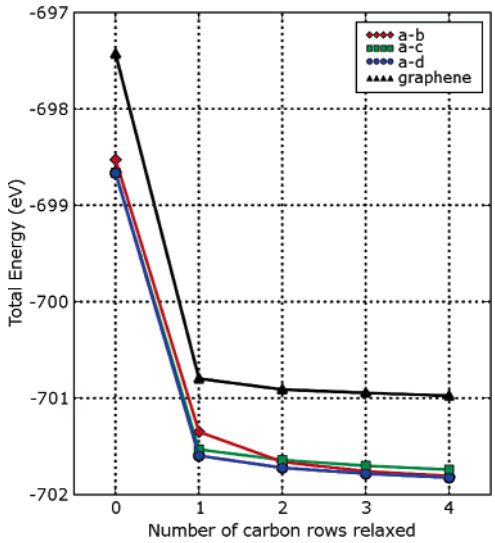

Figure 6. Total energy relaxation vs number of rows of graphene allowed to relax for various configurations of two nitrogen atoms on the edge of graphene, as shown in Figure 5(i).

TABLE 3: Relative Energies and Heats of Substitution for Two Nitrogen Atoms on the Edge of Graphene Sheet (See Figure 5)[a]

positions	relative energy (eV)	heat of substitution (eV)
a−b	0.0 (0.0)	−2.64 (+1.06)
a−c	+0.07 (−0.75)	−2.58 (+0.31)
a−d	−0.01 (−0.88)	−2.66 (+0.18)

[a] The numbers in parentheses are in the presence of hydrogen and others in the absence of hydrogen.

coordination—were also considered. Such configurations were always found to be higher in energy compared to the ones shown in Figure 5 (for in both the presence and absence of hydrogen atoms). The energies associated with nitrogen substitutions in all configurations (as shown in Figure 5(i)) in the absence of hydrogen passivation are exothermic. There is also no repulsive

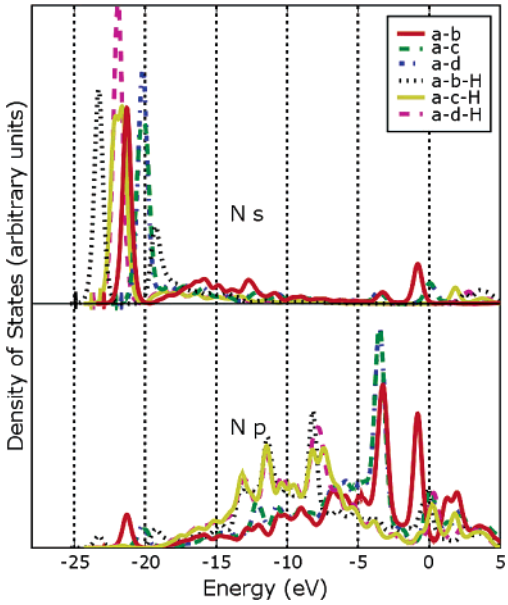

Figure 7. Nitrogen partial density of states for nitrogen substituted on the edge of graphene.

interaction for nitrogen substitution on the edge in this case in contrast to substitutions in the interior. The energies of nitrogen substitution on graphene edge in the presence of hydrogen are endothermic, although the magnitude of endothermcity is small—especially for the lower energy configuration (a−c and a−d). Because these calculations are done at 0 K and entropic effects are not taken into account, this endothermic reaction could be exothermic at room temperature.

It is evident from Tables 2 and 3 that substitution of nitrogen in carbon in the bulk of the graphene sheet is endothermic. On the edge, however, the result depends on the presence or absence of hydrogen. While in the absence of hydrogen the substitution is exothermic, in the presence the substitution is endothermic. In both cases, the nitrogen on edge substitutions would be preferable to the nitrogen substitution in interior. A conclusion from this study is that majority of added nitrogen atoms on graphene sheet are likely to reside at edges, rather interior sites on graphene. Such nitrogen-enriched graphene edges make bonding to iron possible, as proposed by Dodelet and co-workers.[4]

Figure 7 shows the partial DOS for the nitrogen states. For the configurations with no hydrogen passivation, the 2s states are closer to the Fermi level by ∼2 eV. When the nitrogen atoms are farther than second-nearest neighbor, they do not interact with each other, and the 2s states show little or no splitting. In the a−b configuration in the absence of hydrogen passivation, the antibonding 2s states hybridize with the carbon s states and delocalize in energy, while the DOS for same configuration in the presence of hydrogen is similar to the a−b configuration in Figure 3.

The nitrogen 2p DOS for hydrogen-passivated configurations have peaks between ∼14 and ∼8 eV below the Fermi level. This is similar to the peaks of nitrogen 2p in Figure 4. This is very different from the case when the edge is unpassivated. In those configurations, the peaks are closer to the Fermi level at ∼3.5 eV below it. In both cases, the DOS curves for a−c and a−d configurations are similar, indicating that once the nitrogen atoms are beyond second-nearest neighbors, they do not interact with each other. In configuration a−b with no passivation, the nitrogen p states show a peak very close to the Fermi energy.

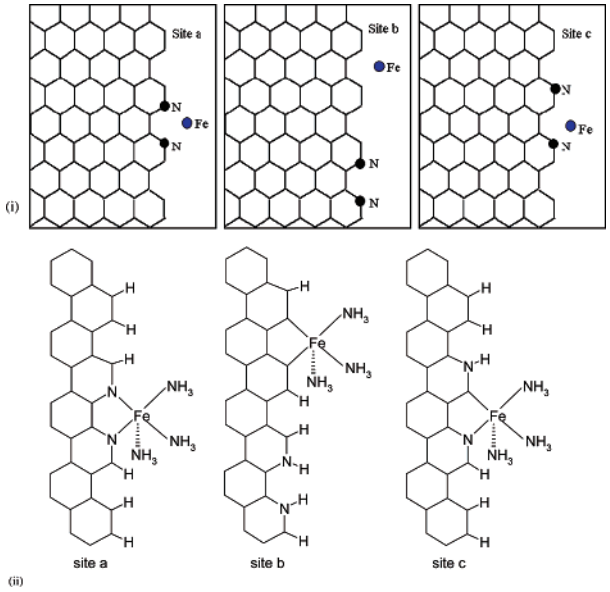

Figure 8. Positions of Fe atoms on the edge of nitrogenated graphene: (i) Fe bond sites a, b, c; (ii) models of nitrided graphene edge being passivated by hydrogen atoms and bonded with Fe. Here Fe is coordinated with three NH_3 ligands.

The ultraviolet photoemission spectroscopy (UPS) of amorphous CN_x materials have been studied by several groups.[14,25−29] Electron energy loss spectra (EELS) for hydrogenated CN_x were measured by Silva and co-workers.[30] From this study, it was found that the 2p DOS of nitrogen has peaks within 5 eV of the Fermi level. When the nitrogen atoms are within the bulk of graphene sheet, the 2p densities of states showed peaks right at the Fermi level, as shown in Figure 4. When the two nitrogen atoms are on the edge of graphene sheet, the 2p densities of states of nitrogen atoms show peaks at 1 or 3.5 eV from the Fermi level, as shown in Figure 7. Souta[25] found that as the concentration of N increases in the sample increases, the UPS peaks at 4.5, 7.1, and 9.5 eV increase, while peaks at 3.6 and 7.7 eV decrease. The peak at 4.5 eV was attributed to the nitrogen lone pair electrons. This assignment is consistent with our DOS results as shown in Figure 7. Santos et al.[14] calculated the DOS for nitrogen-substituted carbon clusters. Their DOS for CN_x clusters also showed a N lone pair peak at ∼5.0 eV. Zhao and co-workers[27] also found that for their a-CN_x sample, as the nitrogen content increased, the UPS peaks at regions 2−7 and 20−30 eV increase. Overall, the DOSs determined for two nitrogen atoms substitution in graphene sheet from this work are in good correspondence with experimental observed UPS data.

Incorporation of Iron on the Edge of Nitrogen-Containing Graphene. The lowest energy configurations from the nitrogen substitution on the edge were chosen, and arrangements of Fe atoms around those configurations were studied. It was assumed that Fe atom would bond on configurations that were thermodynamically the most stable ones. Figure 8 shows the various configurations that were considered. Some other configurations were also considered but were found to be much higher in energy. As shown in Figure 8(i), for the cases considered, the Fe atom was bonded only to two atoms. The effect of ligands on the other side of the Fe atom would be considered separately later.

In the absence of hydrogen atoms passivating the edge, the Fe atom causes substantial relaxation in the graphene sheet. Figure 9 shows the convergence of the total energy in the absence of hydrogen passivation as a function of the numbers

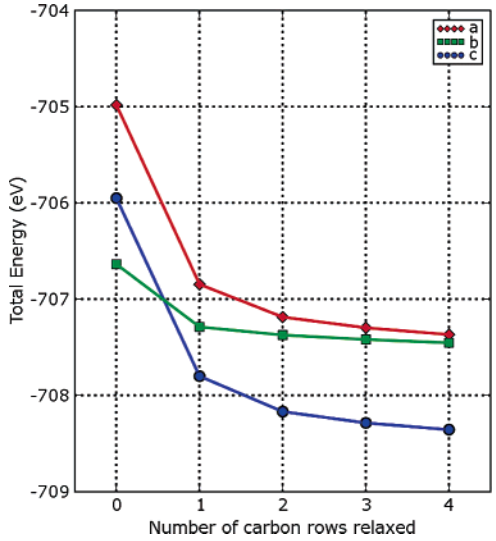

Figure 9. Total energy relaxation vs number of rows of graphene allowed to move for various configurations of Fe and two nitrogen atoms on the edge of graphene, in the absence of hydrogen passivation.

TABLE 4: Relative Energies Position of Fe Atom on the Edge of Nitrided Graphene Sheet (See Figure 8)[a]

positions	relative energy (eV)	relative energy (eV) with ammonia ligands
a	0.00 (0.00)	0.00 (0.00)
b	−0.12 (+2.01)	+0.51(+2.53)
c	−0.99 (+0.33)	−0.73(+0.61)

[a] The values in parentheses are ones in the presence of hydrogen and others without.

of rows of carbon atoms from graphene edge that were relaxed. Table 4 shows the relative stability of three different arrangements of Fe atom on the edge of graphene containing nitrogen atoms. From Table 4, it can be seen that the most stable structure in the absence of hydrogen passivation is the one with Fe attached to a nitrogen atom on the edge and a carbon (site c in Figure 8(i)). This energetically most stable structure (site c in Figure 8(i)) differs from the catalytic site model proposed by Dodelet et al.[4]

In the presence of hydrogen passivation, however, the ordering of configurations according to stability is not the same. Hydrogen atoms can passivate the edge atoms in several different configurations. For each of the configuration in Figure 8(i) several possibilities were considered. It was found that when the nitrogen atoms are not connected to the Fe atom, it is always energetically favorable for the hydrogen atoms to passivate them. This is consistent with the finding above for nitrogen substitution on the edge. In contrast to the relative energetics in the absence of hydrogen passivation, it was found that for the lowest energy configuration the Fe atom was attached to two nitrogen atoms (Figure 8(i), site a).

Figure 10 shows the partial densities of states for the iron in the various configurations in the presence and absence of hydrogen. As can be seen from the figure, Fe s states hybridize to some extent with the valence band. However, in all cases there is also a peak above the Fermi level, indicating that it is partially occupied. The Fe d states have a peak at the Fermi level and are partially occupied. These d states probably play a role in electrocatalysis just as they do in homogeneous catalysis.

It is known that iron is seldom, if ever, just 2-fold coordinated. The relative stability ordering (as shown in Table 4) could change if the coordination number of the iron were higher. Experimentally, electrocatalysts are prepared in a strongly

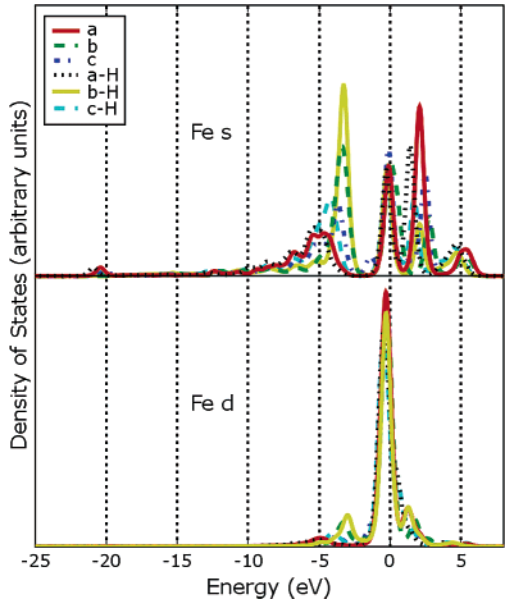

Figure 10. Fe partial density of states for configurations shown in Figure 8.

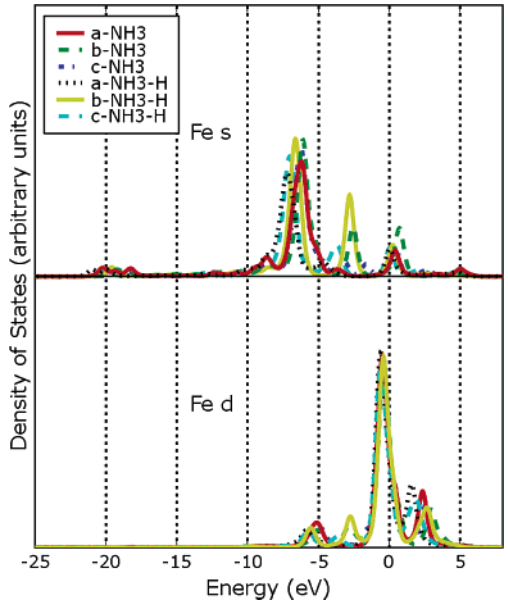

Figure 11. Fe partial density of states for configurations shown in Figure 8.

reducing environment provided by ammonia at high temperature. The Fe atom is not expected to be 2-fold coordinated under such conditions. To assess the role of coordination around the iron atom, we examined the relative energies of the all the configurations by coordinating the Fe atom with three NH_3 ligands in a pyramidal structure,[31] as shown in Figure 8(ii). Ammonia is a ligand that binds strongly to both 0 and +1 iron. In the absence of hydrogen passivation, the configuration c was still found to be lowest in energy (as shown in Table 4). However, configuration b was now found to be higher in energy than configuration a. In the presence of passivation, the configuration a was found to be the lowest in energy.

Figure 11 shows the DOS for the configurations in Figure 8 with ammonia ligands. As can be seen from the figure, the states near the Fermi energy have little Fe s character upon this bonding interaction NH_3. These states now are completely hybridized with the valence band. However, the Fe d states are still close to the Fermi energy and available to participate in catalysis.

These results suggest that the most stable linkages near the catalytic site in the absence of hydrogen are the iron atom bonded to a carbon atom and a nitrogen atom. In more realistic, higher coordination number structures, coordinating of iron by NH_3 groups does not change the relative ordering of stability—the lowest energy structure still contains iron bonded to both nitrogen and carbon. In the presence of hydrogen, however, the catalytic site as proposed by Dodelet[4] and co-workers seems to be the lowest in energy.

IV. Conclusions

Substitution of nitrogen in bulk graphene is energetically endothermic, while on the edge it is exothermic when there is no hydrogen passivation and endothermic in the presence of hydrogen. The energy of substitution becomes less unfavorable as the nitrogen atoms get farther apart in the bulk. In the presence of hydrogen, the energetics of substitution of two nitrogen atoms on the edge are similar within ±0.1 eV (see Table 3). In the presence of hydrogen, the energy of substitution becomes less endothermic as the nitrogen atoms get farther apart on the edge. Nitrogen 2s peaks are a good indicator of the distance between the nitrogen atoms in the bulk. We also show some of the minimum-energy configurations for the incorporation of Fe on the edge of the nitrided graphene sheets. Energetically, when there is no hydrogen passivation on the graphene edge, iron prefers to bond with nitrogen and a carbon atom. When the nitrided graphene edge is passivated by hydrogen, iron prefers to bond with two nitrogen atoms (as shown in Figure 8(i), site a), as proposed by Dodelet et al.[4]

Acknowledgment. M.J. thanks Dr. Radoslav Atanasoski and Dr. David G. O'Neill for useful discussions. This research was supported in part by the U.S. Department of Energy (DOE), Cooperative Agreement DE-FC36-03GO13106. DOE support does not constitute an endorsement by DOE of the views expressed in this presentation.

References and Notes

(1) Sidik, R. A.; Anderson, A. B. *J. Electroanal. Chem.* **2002**, *528*, 69.
(2) Atanasoski, R. T. Annual Progress Report, DOE Hydrogen Program, 2004, pp 392−396.
(3) See e.g.: *J. Phys. Chem. B* **2003**, *107*, 1376; *J. Electrochem. Soc.* **2004**, *151*, A1507 and references therein.
(4) Lefèvre, M.; Dodelet, J. P.; Bertrand, P. *J. Phys. Chem. B* **2000**, *104*, 11238.
(5) Merchant, A. R.; McKenzie, D. R.; McCulloch, D. G. *Phys. Rev. B* **2001**, *65*, 024208-1.
(6) Stafstrom, S. *Appl. Phy. Lett.* **2000**, *77*, 3941.
(7) Hultman, L.; Neidhardt, J.; Hellgren, N.; Sjostrom, H.; Sundgren, J.-E. *MRS Bull.* **2003** (March), 194.
(8) Cunhna, C.; Canuto, S.; Fazzio, A. *Phys. Rev. B* **1993**, *48*, 17 806.
(9) Jungnickel, G.; Stich, P. K.; Frauenheim, Th.; Eggen, B. R.; Heggie, M. I.; Latham, C. D.; Cousins, C. S. G. *Phys. Rev. B* **1998**, *57*, R661.
(10) Lu, Y. F.; He, Z. F.; Ren, Z. M. *J. Appl. Phys.* **1999**, *86*, 5417.
(11) Stumm, P.; Drabold, D. A.; Fedders, F. A. *J. Appl. Phys.* **1997**, *81*, 1289.
(12) Liu, A. Y.; Cohen, M. L. *Phys. Rev. B* **1990**, *41*, 10727.
(13) Sjostrom, H.; Stafstrom, S.; Boman, M.; Sundgren, J. E. *Phys. Rev. Lett.* **1995**, *75*, 1336.
(14) dos Sandos, M. C.; Alvarez, F. *Phys. Rev. B.* **1998**, *58*, 13918.
(15) See e.g.: Bron, M.; Radnik, J.; Fieber-Erdmann, M.; Bogdanoff, P.; Fiechter, S. *J. Electroanal. Chem.* **2002**, *535*, 113.
(16) Perdew, J. P.; Wang, Y. *Phys. Rev. B* **1992**, *45*, 13 244.
(17) Kresse, G.; Hafner, J. *Phys. Rev. B* **1993**, *47*, 558.
(18) Kresse ,G.; Furthmüller, J. *Phys. Rev. B* **1996**, *54*, 11169.
(19) Kresse, G.; Furthmüller, J. *Comput. Mater. Sci.* **1996**, *6*, 15.
(20) Kresse, G.; Joubert, D. *Phys. Rev. B* **1999**, *59*, 1758.
(21) See: Winter, M. www.webelements.com, 2001.
(22) Hult, E.; Hyldgaard, P.; Rossmeisl, J.; Lundqvist, B. I. *Phys. Rev. B* **2001**, *64*, 195414.

(23) Lee, Y.; Kim, S.; Tomanek, D. *Phys. Rev. Lett.* **1997**, *78*, 2393.
(24) See for example: http://srdata.nist.gov/cccbdb/getiso.asp?isof=C4H4N2.
(25) Souto, S.; Pickholz, M.; dos Santos, M. C.; Alvarez, F. *Phys. Rev. B* **1998**, *57*, 2536.
(26) Bhattacharyya, S.; Vallée, C.; Cardinaud, C.; Chauvet, O.; Turban, G. *J. Appl. Phys.* **1999**, *85*, 2162.
(27) Zhao, J. P.; Chen, Z. Y.; Yano, T.; Ooie, T.; Yoneda, M.; Sakakibara, J. *Appl. Phys. A* **2001**, *73*, 97.
(28) Jama, C.; Al khawwam, A.; Loir, A. S.; Goudmand, P.; Dessaux, O.; Gengembre, L.; Grimblot, J, *Surf. Interface Anal.* **2001**, *31*, 815.
(29) Zhou, Z.; Xia, L.; Sun M. *Appl. Surf. Sci.* **2004**, *222*, 327; *Appl. Surf. Sci.* **2003**, *210*, 293.
(30) Silva, S. R. P.; Robertson, J.; Amaratunga, G. A. J.; Rafferty, B.; Brown, L. M.; Schwan, J.; Franceschini, D. F.; Mariotto, G. *J. Appl. Phys.* **1997**, *81*, 2626.
(31) Anderson, A. B.; Sidik, R. A. *J. Phys. Chem. B* **2004**, *108*, 5031.
(32) Herzberg, G. *Phys. Rev. Lett.* **1969**, *23*, 1081.
(33) Tureèek, F. *J. Mass Spectrom.* **1998**, *33*, 779.
(34) See for example: Hwang, D. K.; Kim, K.; Kim, J. H.; Im, S.; Jung, D. Y.; Kim, E. *Appl. Phys. Lett.* **2004**, *85*, 5568.
(35) Bouchet-Fabre, B.; Godet, C.; Larceda, M.; Charvet, S.; Zellama, K.; Ballutaud, D. *J. Appl. Phys.* **2004**, *95*, 3427.